ARTICLES

Journal of Semiconductors
(2022) 43, 112301
doi: 10.1088/1674-4926/43/11/112301

Four-channel CWDM transmitter chip based on thin-film lithium niobate platform

Kaixuan Chen[1, 2], Gengxin Chen[3], Ziliang Ruan[3], Xuancong Fan[1, 2], Junwei Zhang[4], Ranfeng Gan[1], Jie Liu[4], Daoxin Dai[3, 5], Changjian Guo[1, 2], and Liu Liu[3, 5, †]

[1]Guangdong Provincial Key Laboratory of Optical Information Materials and Technology, South China Academy of Advanced Optoelectronics, South China Normal University, Higher-Education Mega-Center, Guangzhou 510006, China

[2]National Center for International Research on Green Optoelectronics, South China Normal University, Guangzhou 510006, China

[3]State Key Laboratory for Modern Optical Instrumentation, College of Optical Science and Engineering, International Research Center for Advanced Photonics, Zhejiang University, Hangzhou 310058, China

[4]State Key Laboratory of Optoelectronic Materials and Technologies, School of Electronics and Information Technology, Sun Yat-Sen University, Guangzhou 510006, China

[5]Jiaxing Key Laboratory of Photonic Sensing & Intelligent Imaging, Intelligent Optics & Photonics Research Center, Jiaxing Research Institute, Zhejiang University, Jiaxing 314000, China

Abstract: Multi-lane integrated transmitter chips are key components in future compact optical modules to realize high-speed optical interconnects. Thin-film lithium niobate (TFLN) photonics have emerged as a promising platform for achieving high-performance chip-scale optical systems. Combining a coarse wavelength-division multiplexing (CWDM) devices using fabrication-tolerant angled multimode interferometer structure and high-performance electro-optical modulators, we demonstrate monolithic on-chip four-channel CWDM transmitter on the TFLN platform for the first time. The four-channel CWDM transmitter enables high-speed transmissions of 100 Gb/s data rate per wavelength channel (i.e., an aggregated date rate of 400 Gb/s).

Key words: transmitter; lithium niobate; coarse wavelength-division multiplexing; electro-optic modulator

Citation: K X Chen, G X Chen, Z L Ruan, X C Fan, J W Zhang, R F Gan, J Liu, D X Dai, C J Guo, and L Liu, Four-channel CWDM transmitter chip based on thin-film lithium niobate platform[J]. *J. Semicond.*, 2022, 43(11), 112301. https://doi.org/10.1088/1674-4926/43/11/112301

1. Introduction

With the rapid growth of data traffic in local area networks, wireless mobile communications, and data centers[1], high speed, low-cost, and highly compact transceivers have attracted considerable interest in recent years. In order to exploit the data transmission capacity of an optical connection, wavelength-division multiplexing (WDM) and parallel single-mode fiber 4-lane (PSM4)[2] are mainly adopted. In these applications, a multi-lane transmitter optical sub-assembly (TOSA), with integration of lasers, modulators, and WDM filters, can help miniaturize an optical transceiver. Recent integration technologies for multi-lane TOSA, such as thin-film filter assembling[3], indium phosphide based integration[4, 5], silicon photonic integrated circuits[6], and planar lightwave circuit based hybrid integrated[7], have been extensively studied and adopted in practical applications. Among then, silicon photonics integration is a highly promising platform for next-generation optical interconnect devices, due to its small footprint, low power, and complementary metal–oxide–semiconductor compatibility[8]. Meanwhile, in order to realize a higher bit rate (e.g., 200 Gb/s per wavelength) the simple on-off keying (OOK) signal format may no longer be a viable approach because the expected electro-optic (EO) bandwidths for the modulator and the photo-detector in this case need to be more than 100 GHz[9], which could be a huge challenge for the device design. Therefore, advanced modulation formats, such as multi-level pulse amplitude modulation (PAM), quadrature amplitude modulation, discrete multi-tone modulation, are considered and have been widely investigated[10, 11]. Considering these aspects, a four-channel silicon photonic transmitter operating at an aggregated data rate of 800 Gb/s is demonstrated[8], but with a complex co-design and co-optimization together with the driver due to the limited bandwidth of a silicon modulator.

Thin-film lithium niobate (TFLN) platform[12] has emerged recently as a new photonic integration platform for optical communications[13], quantum photonics[14], and microwave photonics[15], due to its excellent material properties, including linear Pockels effect, wide transparent window, and excellent temperature stability. High-speed EO modulator, a key functional component of an optical transmitter, has been proposed using different kinds of configurations on the TFLN platform, such as Mach-Zehnder interferometer (MZI) modulators[16], Michelson interferometer modulators[17], Brag grating modulators[18], Fabry-Perot modulators[19], with a possible bandwidth of >100 GHz and insertion loss of <1 dB. Recently, a high-power PSM4 transmitter on the TFLN platform employing an external flip-chip bonded distributed feedback laser is demonstrated[20], showing an EO bandwidth of 50 GHz with a half-wave voltage V_π of 4.3 V for each channel.

In this paper, an monolithic four-channel coarse WDM

Correspondence to: L Liu, liuliuopt@zju.edu.cn
Received 11 APRIL 2022; Revised 21 JUNE 2022.

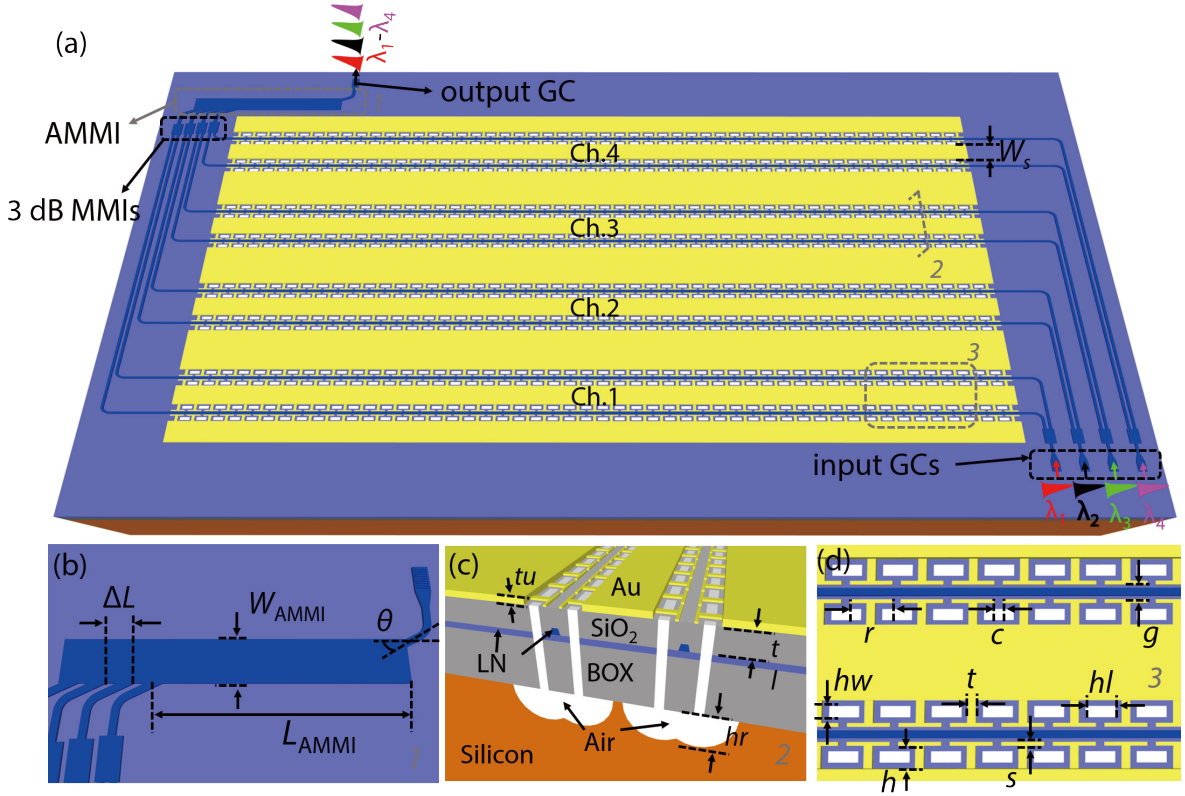

Fig. 1. (Color online) (Color online) Proposed four-channel CWDM transmitter on the TFLN platform. 3D view of (a) whole structure and (b) CWDM device based on the AMMI structure. (c) Cross-sectional view of the modulation section. (d) Top view of the CLTW electrode.

(CWDM) transmitter chip on the TFLN platform is demonstrated, which includes an CWDM device using angled multimode interferometer (AMMI) structure[21] and four MZI modulators[22]. Such a TFLN based CWDM device exhibits a compact size and a large fabrication tolerance. The MZI modulators here employ a periodic capacitively-loaded travelling (CLTW) electrode design, and exhibit an excellent modulation performance with a half-wave voltage of ~1.7 V and an EO bandwidth of >40 GHz for each channel. 256 Gb/s (4 × 64 Gb/s) OOK signal transmission and 400 Gb/s (4 × 100 Gb/s) PAM-4 signal transmission are experimentally demonstrated.

2. Transmitter design and fabrication

Fig. 1(a) shows a three-dimensional (3D) view of the proposed four-channel CWDM transmitter on the TFLN platform, which integrates a four-channel CWDM device and four EO modulators (Ch. 1-Ch. 4). External laser lights at a standard CWDM grid (i.e., 1271, 1291, 1311, and 1331 nm) are coupled in the transmitter using four grating couplers (GCs), respectively, whose peak coupling efficiencies are aligned to the wavelengths of the corresponding channels in order to obtain the highest signal light. The four input GCs and a common output GC are designed with periods of 737, 747, 756, 764, and 752 nm and gaps of 516, 500, 476, 458, and 500 nm, respectively. With the help of the integrated CWDM device of the AMMI structure, the laser lights after modulation from the 4 channels are then combined and coupled out through a common GC. Compared to traditional CWDM structures, such as array-waveguide grating, cascaded MZI, or planar concave gratings, the AMMI structure here maintains a higher fabrication tolerance[21], and avoids bending waveguides, which are difficult to design in the anisotropic TFLN platform[23]. The TFLN waveguide has a ridge height of 200 nm, (i.e., half of the total LN thickness). As shown in Fig. 1(b), the width of the AMMI structure W_{AMMI} is 17.54 μm and the length L_{AMMI} is optimized as 1943 μm. The tilted angle θ and channel distance ΔL are set as 0.17 rad and 37 μm, respectively, to ensure a filtered wavelength spacing of 20 nm, as well as a low insertion loss (IL) and a small crosstalk. More details on the design of this AMMI based CWDM device can be found in Ref. [21].

For the modulators here, a balanced MZI structure with a push-pull electrode configuration is adopted. 3dB multimode interferometer couplers are used as the light splitter and combiner. In the modulation sections, the TFLN waveguide has a width of 1.5 μm, and the CLTW electrode with a periodic T-segment structure is adopted, which has been shown to present a good voltage-bandwidth product for modulation[22, 24]. The width of the unloaded signal electrode is set large enough as 75 μm to ensure low radio-frequency (RF) conductor loss, and the periodic T-segment structure can effectively block the electrical current flow perpendicular to the electrode, and keep the distributed capacitance constant. In order to achieve velocity matching between RF and optical waves, the substrate undercut etching technique is introduced, as shown in Fig. 1(c). The detailed parameters of the whole modulator structure are given as (*r*, *c*, *s*, *t*, *h*, *g*, *hw*, *hl*, *tl*, *tu*, *hr*) = (47, 3, 2, 5, 15, 1.6, 9, 39, 0.9, 1.1, 35) μm, as also shown in Figs. 1(c) and 1(d). A high modulation efficiency (i.e., a half-wave-voltage-length product of $V_\pi L$ = 1.54 V·cm) can be obtained without introducing any additional optical absorption losses from the electrodes.

The four-channel CWDM transmitter is fabricated on an x-cut lithium niobate-on-insulator wafer from NANOLN,

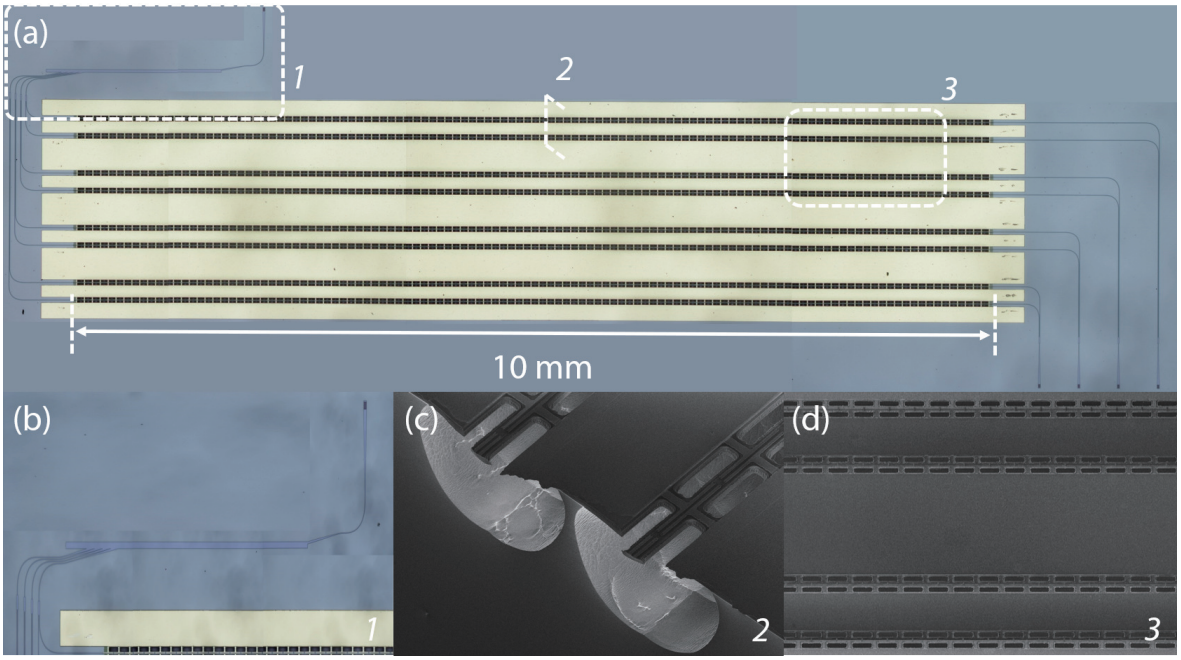

Fig. 2. Optical images of (a) whole transmitter and (b) four-channel CWDM device. Scanning electron microscope images of (c) cross-sectional view and (d) top view of the modulation section.

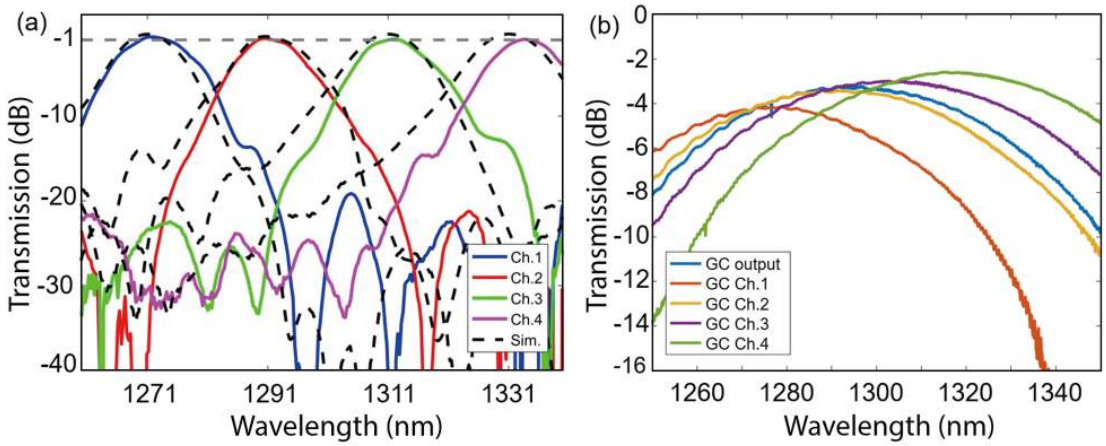

Fig. 3. (Color online) (a) Measured and simulated transmission spectral responses of the fabricated CWDM device. (b) Measured transmission spectral responses of the four input GCs and the common output GC.

where a 400 nm thick LN film is bonded on a 3 μm buried oxide (BOX). The waveguide and GC patterns were defined using an electro-beam lithography system (Raith Voyager), and 200 nm thick lithium niobate was etched using an inductively coupled plasma reactive ion etching (ICP-RIE) process. A SiO_2 over-cladding layer was deposited using plasma enhanced chemical vapor deposition. Then, holes between the T-segment structures were patterned using ultra-violet contact lithography, and the SiO_2 cladding layer, the lithium niobate slab layer, and the BOX layer were etched in turn to expose the silicon substrate. Next, the CLTW electrode made of gold was fabricated using lift-off processes. Finally, the holes were patterned again, and silicon etching using the ICP-RIE technology was performed to remove the silicon substrate beneath the modulator waveguides. An SF_6 based chemistry with no bias power was used for the isotropic silicon dry-etching. The etching selectivity of such a recipe to photoresist and SiO_2 are therefore high. Fig. 2 shows some optical images and scanning electron microscope images of the fabricated transmitter chip.

3. Transmitter measurement

The CWDM device and GCs was first characterized using a separated testing structure. The measured and simulated spectral responses of the device are shown in Fig. 3(a). One can see that the present CWDM device exhibits a 3 dB bandwidth of 12 nm, an IL of <0.9 dB, and an averaged crosstalk of 18.15 dB at the peak wavelengths, which are also well matched to the simulated results. The losses of the four input GCs and the output GC at their central wavelengths are 4.2, 3.4, 3, 2.6, and 3 dB, respectively, as shown in Fig. 3(b). The fabricated four-channel CWDM transmitter including four modulators of a modulation section length of 10 mm as shown in Fig. 2(a) was then measured. Four-channel laser lights at the corresponding CWDM wavelengths were coupled in the chip through four GCs. The on-chip losses are 3.15, 2.75, 3.44, and 1.52 dB for Ch. 1 to Ch. 4, respectively, which includes the losses of the modulator and the CWDM device. Fig. 4 shows the half-wave voltage V_π measurements for the four modulators using a 100 kHz triangular voltage

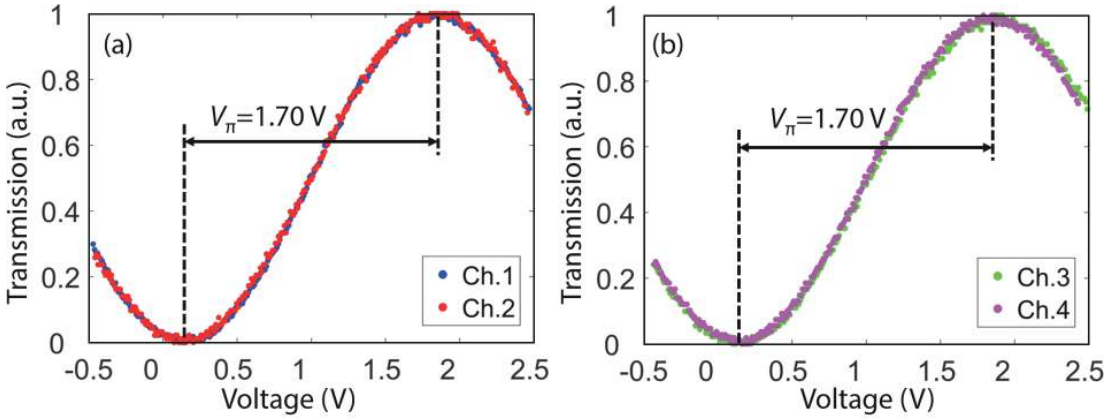

Fig. 4. (Color online) Normalized optical transmission of the fabricated four modulators as a function of the applied voltage for (a) Ch. 1 and Ch. 2, and (b) Ch. 3 and Ch. 4.

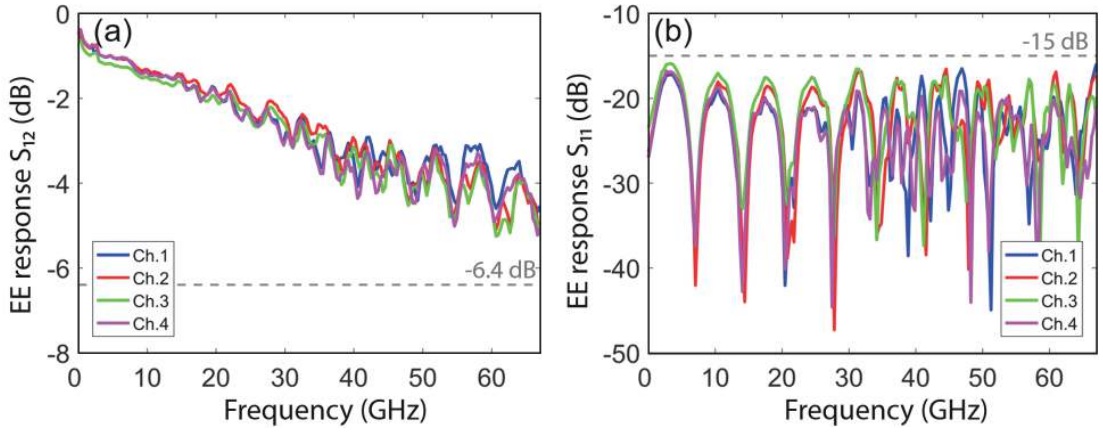

Fig. 5. (Color online) Measured EE (a) transmissions S_{12} and (b) reflections S_{11} for the four modulators.

sweep. The values of V_π are 1.68, 1.70, 1.66, and 1.70 V for Ch. 1 to Ch. 4, respectively, which indicates a good uniformity for the four modulators. However, the imbalanced insertion losses measured here for the four channels mainly come from slight misalignments of CWDM wavelengths to the laser lights.

For high-speed performances of the modulators, the employed CLTW electrode is expected to give a low microwave loss. The electric-electric (EE) S_{12} and S_{11} responses of the electrode were measured using a vector network analyzer (VNA). Before measurements, the VNA, together with the microwave probes, was first calibrated using a ground-signal-ground calibration kit. As shown in Figs. 5(a) and 5(b), the measured EE responses for the four modulators show a similar trend with transmissions of <–6.4 dB (i.e., a level corresponding to the 3 dB EO bandwidth for an index and impedance matched travelling wave modulator[22]), and reflections of <–15 dB within 67 GHz frequency.

In the present chip, electrodes in adjacent channels are placed side by side with a pitch of 350 μm, which might induce unwanted microwave crosstalks. The same VNA was used to test the EE crosstalk characteristic of the fabricated four-channel CWDM transmitter. As for Ch. *X*, the crosstalk response can be measured by connecting the input and output RF ports of the VNA to Ch. *Y* and Ch. *X* (*X*, *Y* = 1, 2, 3, 4), respectively. The normalized crosstalk from Ch. *Y* to Ch. *X* can be calculated by subtracting the EE transmission response of Ch. *X* shown in Fig. 5(a). As shown in Figs. 6(a)–6(d), the measured crosstalks become worse at higher frequencies, and are higher from adjacent channels than those from non-adjacent ones. Generally, the crosstalks are maintained less than –10 dB for frequencies of <40 GHz for all the four channels.

Next, the small-signal EO modulation responses S_{12} of the fabricated CWDM transmitter were measured as shown in Fig. 7. The driving signal was fed into the modulator using one microwave probe on one side of the CLTW electrode, and the 50 Ω termination is applied on the other side with another probe. The modulated light was detected using a high-speed photodiode (PD, Finisar XPDV3120) with a bandwidth of 70 GHz and a responsivity of 0.25 A/W at O-band. It can be observed that the 3 dB EO bandwidths for all channels are better than 40 GHz. The fluctuations beyond 40 GHz are due to the limited responsivity of the PD and the lack of an optical pre-amplifier before detection, which limits the signal-to-noise in measurements here. A simulated EO response is also included in Fig. 7 using the measured electrode parameters in Fig. 5, which indicates that the expected 3-dB EO bandwidth should be larger than 67 GHz.

The data transmission performances using the fabricated transmitter were also tested with a setup shown in Fig. 8(a). A pseudo-random bit sequence (PRBS) with a length of 2^{15}–1 were generated using a 256 GS/s arbitrary waveform generator (AWG, Keysight M8199A) with an analog bandwidth of 70 GHz. The PRBS signal was amplified by a linear RF

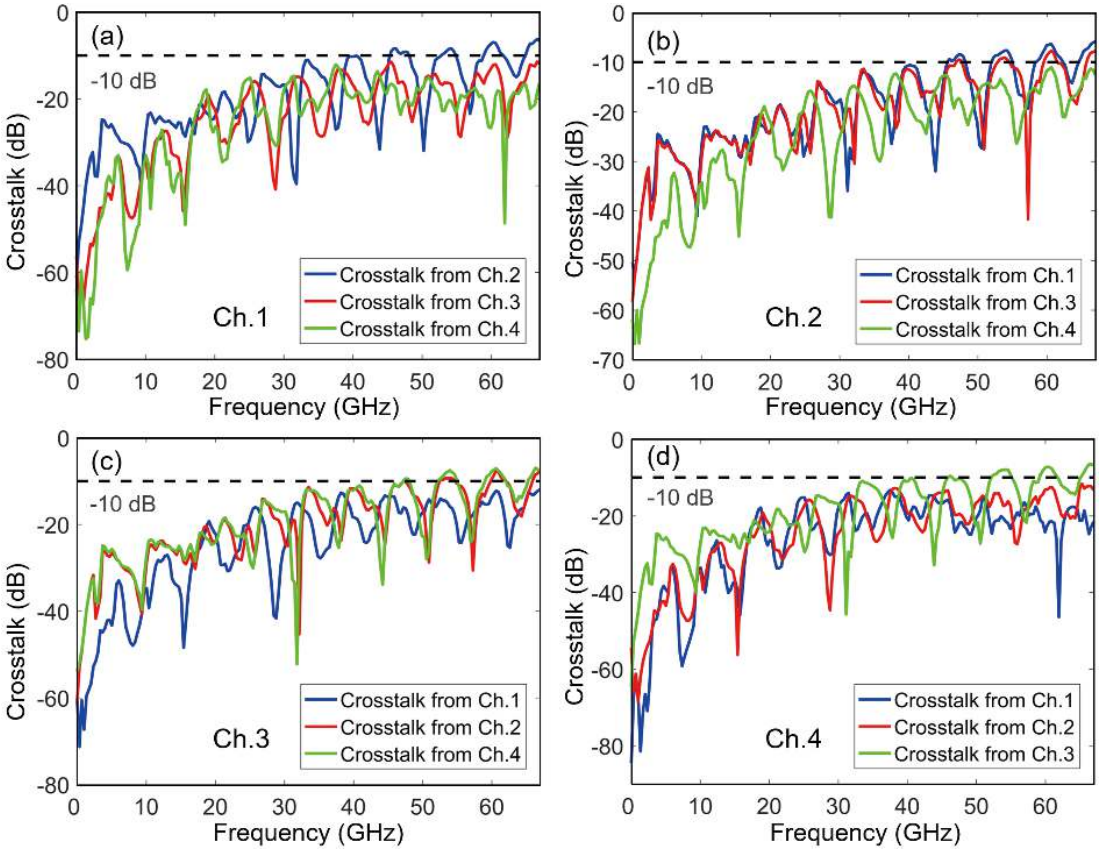

Fig. 6. (Color online) Measured EE crosstalk characteristics of the fabricated CWDM transmitter for (a) Ch. 1, (b) Ch. 2, (c) Ch. 3, and (d) Ch. 4.

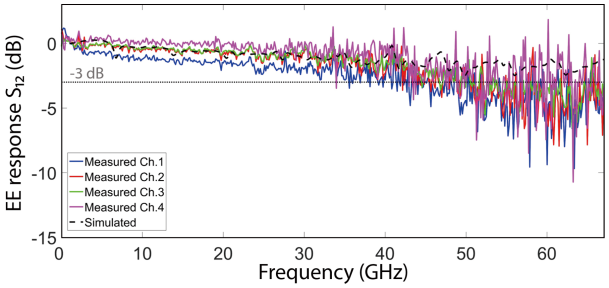

Fig. 7. (Color online) Measured and simulated EO responses for the four modulators.

amplifier (SHF 807) to a peak-to-peak voltage of ~1.41 V, and fed to the fabricated device together with a direct-current bias through a bias-T. The modulated light was directly detected by the high-speed PD without any optical pre-amplifier. Finally, the eye diagrams were recorded using a sampling oscilloscope (Agilent 86100D) with a bandwidth of 80 GHz. The eye diagrams for 64 Gb/s OOK signal in the four channels of the CWDM transmitter are shown in Figs. 8(b)–8(e) with good eye openings. By adjusting the bias voltages, the best dynamic extinction ratios (ERs) of 6.1, 7.3, 8.2 and 5.8 dB can be achieved for Ch. 1 to Ch. 4, respectively. Moreover, the eye diagrams for 100 Gb/s (50 GBaud) PAM-4 signal for the four channels are also shown in Figs. 9(a)–9(d). Good eye openings are observed for Ch. 2 and Ch. 3, while for Ch. 1 and Ch. 4 the eye diagrams are worse. This might be due to the limited coupling wavelength bandwidth of the output GC, which exhibits relatively large coupling losses for Ch. 1 and Ch. 4 wavelengths. Using a broadband edge coupler with higher coupling efficiencies[25] to reduce the optical coupling loss can improve the quality of eye diagrams at 100 Gb/s.

4. Conclusion

In summary, we have introduced a compact monolithically integrated on-chip four-channel CWDM transmitter on the TFLN platform. The CWDM device is based on the AMMI structure, which enables an ultra-low insertion loss of <0.9 dB, 3 dB bandwidth of 12 nm, and averaged crosstalk of 18.15 dB for the four standard CWDM channels. The EO modulators are included in the chip using a CLTW electrode, which helps achieve an EO modulation bandwidth of >40 GHz, and enables 100 Gb/s PAM-4 signal transmission. The demonstrated on-chip four-channel CWDM transmitter on the TFLN platform will be a viable solution for 400 G and future 800 G-1.6 T optical transceiver applications to achieve high-speed optical interconnects.

Acknowledgements

This work is supported partially by the National Major Research and Development Program (2019YFB1803902), National Natural Science Foundation of China (NSFC) (62135012, 62105107), Leading Innovative and Entrepreneur Team Introduction Program of Zhejiang (2021R01001), Guangdong Basic and Applied Basic Research Foundation (2021A 1515012215, 2021B1515120057), Science and Technology Planning Project of Guangdong Province (2019A050510039), and Fundamental Research Funds for the Central Universities (2021QNA5001).

References

[1] Winzer P J, Neilson D T, Chraplyvy A R. Fiber-optic transmission and networking: the previous 20 and the next 20 years. Opt Ex-

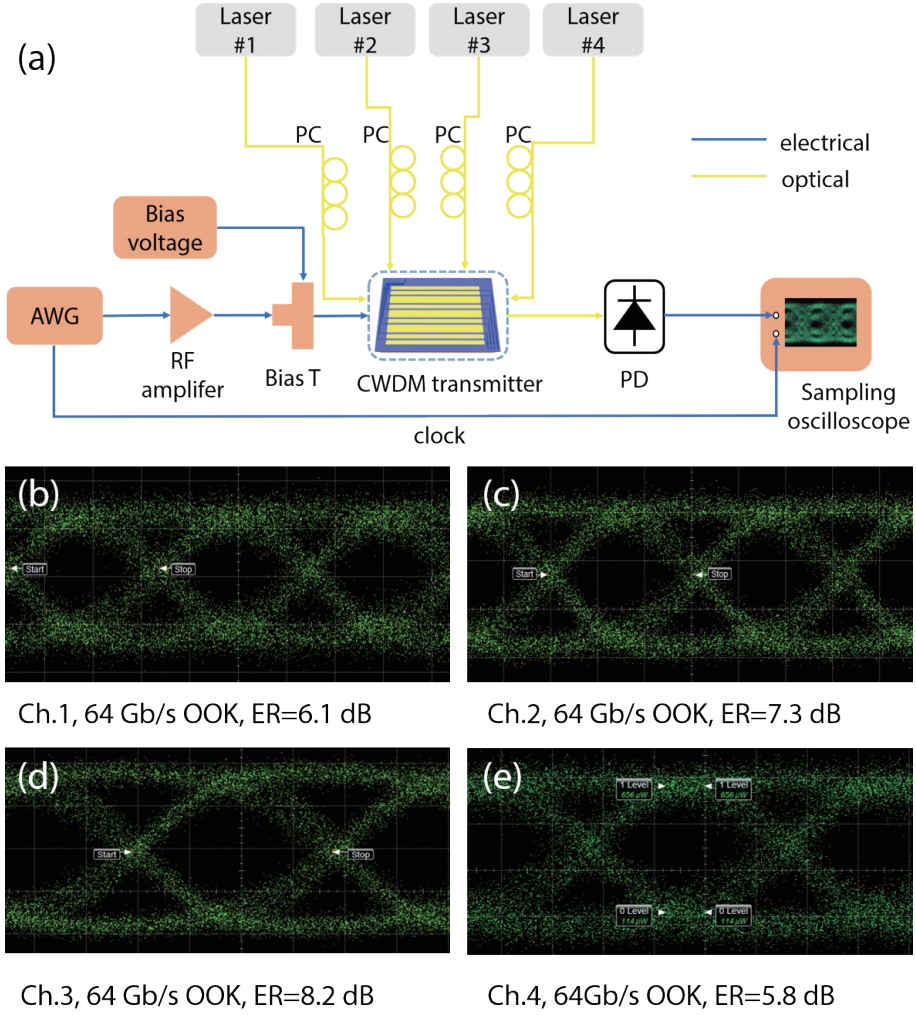

Fig. 8. (Color online) (a) Experimental setup for high-speed data transmission measurements. PC: polarization controller. Measured optical eye diagrams for the OOK format at a data rate of 64 Gb/s for (b) Ch. 1, (c) Ch. 2, (d) Ch. 3, and (e) Ch. 4.

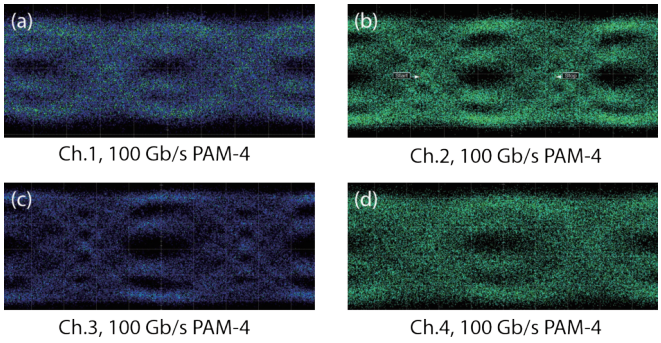

Fig. 9. (Color online) Measured optical eye diagrams for the PAM-4 format at a data rate of 100 Gb/s for (a) Ch. 1, (b) Ch. 2, (c) Ch. 3, and (d) Ch. 4.

press, 2018, 26(18), 24190

[2] Liu J, Ye Y, Deng L, et al. Integrated four-channel directly modulated O-band optical transceiver for radio over fiber application. Opt Express, 2018, 26(17), 21490

[3] Arima R, Yamashita T, Yahagi T, et al. Demonstration of world-first 103 Gbit/s transmission over 40 km single mode fiber by 1310 nm LAN-WDM optical transceiver for 100GbE. National Fiber Optic Engineers Conference, 2011, JWA9

[4] Fujisawa T, Kanazawa S, Ishii H, et al. 1.3-μm × 25-Gb/s monolithically integrated light source for metro area 100-Gb/s ethernet. IEEE Photonics Technol Lett, 2011, 23(6), 356

[5] Kanazawa S, Fujisawa T, Ohki A, et al. A compact EADFB laser array module for a future 100-Gb/s Ethernet transceiver. IEEE J Sel Top Quantum Electron, 2011, 17(5), 1191

[6] Ramaswamy A, Roth J, Norberg E J, et al. A WDM 4× 28Gbps integrated silicon photonic transmitter driven by 32nm CMOS driver ICs. Optical Fiber Communication Conference, 2015, Th5B.5

[7] Murao T, Yasui N, Shinada T, et al. Integrated spatial optical system for compact 28-Gb/s × 4-lane transmitter optical subassemblies. IEEE Photonics Technol Lett, 2014, 26(22), 2275

[8] Zhang H, Li M, Zhang Y, et al. 800 Gbit/s transmission over 1 km single-mode fiber using a four-channel silicon photonic transmitter. Photonics Res, 2020, 8(11), 1776

[9] Mardoyan H, Jorge F, Ozolins O, et al. 204-GBaud on-off keying transmitter for inter-data center communications. Optical Fiber Communication Conference, 2018, Th4A.4

[10] Zhong K, Zhou X, Huo J, et al. Digital signal processing for short-reach optical communications: A review of current technologies and future trends. J Lightwave Technol, 2018, 36(2), 377

[11] Motaghiannezam S. Optical PAM4 signaling and system performance for DCI applications. Optical Fiber Communication Conference, 2019, M3A.1

[12] Zhu D, Shao L, Yu M, et al. Integrated photonics on thin-film lithium niobate. Adv Opt Photonics, 2021, 13(2), 242

[13] Wooten E L, Kissa K M, Yi-Yan A, et al. A review of lithium niobate modulators for fiber-optic communications systems. IEEE J Sel Top Quantum Electron, 2000, 6(1), 69

[14] Saravi S, Pertsch T, Setzpfandt F. Lithium niobate on insulator: An emerging platform for integrated quantum photonics. Adv Opt Mater, 2021, 9(22), 2100789

[15] Marpaung D, Yao J, Capmany J. Integrated microwave photonics. Nat Photonics, 2019, 13(2), 80
[16] Wang C, Zhang M, Chen X, et al. Integrated lithium niobate electro-optic modulators operating at CMOS-compatible voltages. Nature, 2018, 562(7725), 101
[17] Jian J, Xu M, Liu L, et al. High modulation efficiency lithium niobate Michelson interferometer modulator. Opt Express, 2019, 27(13), 18731
[18] Pohl D, Messner A, Kaufmann F, et al. 100-Gbd waveguide Bragg grating modulator in thin-film lithium niobate. IEEE Photonics Technol Lett, 2020, 33(2), 85
[19] Xu M, He M, Zhu Y, et al. Integrated thin film lithium niobate Fabry–Perot modulator. Chin Opt Lett, 2021, 19(6), 060003
[20] Shams-Ansari A, Renaud D, Cheng R, et al. Electrically-pumped high-power laser transmitter integrated on thin-film lithium niobate. arXiv preprint arXiv: 2111.08473, 2021
[21] Chen G, Ruan Z, Wang Z, et al. Four-channel CWDM device on a thin-film lithium niobate platform using an angled multimode interferometer structure. Photonics Res, 2022, 10(1), 8
[22] Chen G, Chen K, Gan R, et al. High performance thin-film lithium niobate modulator on a silicon substrate using periodic capacitively loaded traveling-wave electrode. APL Photonics, 2022, 7(2), 026103
[23] Wang J, Chen P, Dai D, et al. Polarization coupling of X-cut thin film lithium niobate based waveguides. IEEE Photonics J, 2020, 12(3), 1
[24] Kharel P, Reimer C, Luke K, et al. Breaking voltage–bandwidth limits in integrated lithium niobate modulators using micro-structured electrodes. Optica, 2021, 8(3), 357
[25] Ying P, Tan H, Zhang J, et al. Low-loss edge-coupling thin-film lithium niobate modulator with an efficient phase shifter. Opt Lett, 2021, 46(6), 1478

Kaixuan Chen obtained his BS degree in 2012 at Guangdong University of Technology, MA. Sc degree in 2016 at South China Normal University, and PhD degree in 2020 at Zhejiang University. In July 2020, he joined South China Normal University as a postdoc. His research interests include silicon photonics and thin-film lithium niobate integrated devices.

Liu Liu obtained his PhD degree in Photonics at the Royal Institute of Technology, Sweden, in 2006, and joined Zhejiang University as a professor in 2020. Before that, he worked as an assistant professor at Technical University of Denmark, Denmark, and as a professor at South China Normal University (SCNU), China. He also served as a vice dean of South China Academy of Advanced Optoelectronics, SCNU, and the director of Guangdong Provincial Research Center for Optical and Electromagnetic Sensing Technologies. His current research interests include silicon photonics and thin-film lithium niobate integrated devices.